Construction and Building Materials 454 (2024) 138996

Contents lists available at ScienceDirect

Construction and Building Materials

journal homepage: www.elsevier.com/locate/conbuildmat

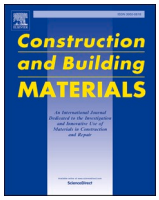

Improving PEG confinement in smart aggregates for lime-based mortars

Paulina Guzmán García Lascurain [a,*], Mariaenrica Frigione [b], Antonella Sarcinella [b], Fátima Linares [c], Laurenz Schröer [d], Veerle Cnudde [d,e], Lucia Toniolo [a], Sara Goidanich [a]

[a] Department of Chemistry, Materials and Chemical Engineering "Giulio Natta", Politecnico di Milano, Milan 20133, Italy
[b] Innovation Engineering Department, University of Salento, Prov.le Lecce-Monteroni, Lecce 73100, Italy
[c] X-Ray Microtomography Service, Scientific Instrumentation Center, University of Granada, Granada 18071, Spain
[d] PProGRess-UGCT, Department of Geology, Ghent University, Ghent, Belgium
[e] Environmental Hydrogeology, Department of Earth Sciences, Utrecht University, Utrecht, the Netherlands

ARTICLE INFO

Keywords:
Phase change materials
FS-PCM confinement
Lime-based mortars
Micro-FTIR mapping
X-ray micro-computed tomography (micro-CT)

ABSTRACT

The implementation of polymer-based Phase Change Materials (PCMs) as functional sustainable aggregates in lime-based mortars has proven to be a viable solution to give a higher thermal performance to historical buildings in the Mediterranean region. To this purpose, PEG-1000 has been selected and used for the impregnation of porous Lecce stone aggregates. However, the inclusion of such impregnated aggregates leads to a drastic reduction of the mechanical properties of the lime-based mortars. The reason behind this reduction may be related both to a lack of compatibility among impregnated aggregates and binder, and to a pour confinement of PEG-1000. These aspects are investigated in the present work, showing that a poor confinement of the PEG-1000 within the aggregates results into its dispersion and mixture with the binder. To prevent this, a simple coating methodology of the functional aggregate particles is proposed, based on the coverage with compatible materials. Five different types of mineral covers were tested: calcium hydroxide, milk of lime, natural hydraulic lime, cocciopesto and pozzolana. Both coated functional aggregates and derived lime mortars were analyzed with a multi-analytical approach. The overall assessment allowed to conclude that the aggregates coated with calcium hydroxide are the best performing and promising ones to confine the PEG-1000 inside the aggregates and potentially increment the mechanical properties of the mortar.

1. Introduction

The current environmental crisis motivates researchers to find innovative solutions to reduce the high levels of emissions, without entirely compromising the economy and human comfort. Particularly, the construction industry is one of the main contributors to the global energy consumption (37 %) and CO_2 emissions (27 %) [1]. These values correspond to the whole lifetime of a building (raw material extraction, construction, use, demolition, waste disposal). Thus, restoration and renovation of buildings with historical value allows to considerably reduce the emissions by extending their lifetime, while contributing to the preservation of the historical value of cities. In summary, restoration and renovation should be seen as prominent solutions to reduce the environmental impact of the construction industry [2,3]. Moreover, a large part of the emissions corresponds to the use-phase, associated in part to heating and cooling systems, especially for buildings with poor thermal efficiency [4]. It is estimated that 30–60 % of energy use could be saved if thermal-efficiency refurbishment is applied to a building [5].

Restoring historical buildings requires the use of compatible materials that do not induce damage to the original masonry. The compatibility of a repair material is evaluated case by case including both esthetical and technical considerations (physical, chemical, and mechanical) [6]. Particularly, for the restoration of buildings constructed before the mid 19th century, lime-based mortars are preferred [7,8]; these are applied to replace or integrate renders and plasters and used for the restoration of brick and stone masonries. The interest of architects and conservators for improving energy efficiency and thermal comfort of historical buildings has risen, especially considering the use of built heritage for public functions, including museums, libraries, universities, theaters, amongst many others. The specific conservation requirements for historical building complicate the use of conventional thermal insulating systems. For example, external thermal retrofitting is often discouraged since it can affect the historical and esthetical value of the facades [9,10]. On the other hand, internal insulation, which is often

* Correspondence to: Piazza Leonardo da Vinci 32, Milano 20133, Italy.
E-mail address: paulina.guzman@polimi.it (P. Guzmán García Lascurain).

https://doi.org/10.1016/j.conbuildmat.2024.138996
Received 13 June 2024; Received in revised form 15 October 2024; Accepted 29 October 2024

characterized by a reduced permeability, may impact the moisture transport dynamics of the historic walls. An over accumulation of moisture in the building's envelop can result in the decay of the historical masonry, such as the increment of frost damage and development of mold [9,10]. Thus, different strategies have been proposed throughout the years to overcome this issue, like the use of Thermal Energy Storage (TES) systems, particularly Phase Change Materials (PCM's) [11–17].

In the past decade, TES systems have risen as a promising solution to be implemented in construction. These systems permit to accumulate thermal energy for a period and release it when it is needed [17,18], thus using the naturally available thermal energy in a more efficient way. One of the most prominent TES are Phase Change Materials (PCMs), which are passive systems that melt and solidify at specific temperatures and store/release energy trough the physical change in phase [4,19]. These transition temperatures depend on each material and can correspond for example to the day and night cycles. Various materials can serve as active PCMs providing a wide versatility to such thermal storage systems.

Their application in construction requires that the used PCM has a relatively stable volume during the phase change (i.e., it does not swell or shrink excessively), the PCM also needs to be compatible with the construction materials to prevent degradation, it should be non-toxic for humans and the environment, easily recyclable, abundant, and economic [4]. PCMs can be incorporated in any element of the building's envelop, each with their own advantages and drawbacks. Particularly, the incorporation into the masonry system permits the use of a big surface for thermal exchange and exploits the versatility of mortars to accommodate the different incorporation methods of PCM [20]. In practice there are four ways to incorporate PCMs: direct impregnation, encapsulation (micro or macro), shape stabilization and form stabilization (vacuum impregnation) [20,21]. The latter consists in the integration of the PCM into an inert porous matrix, thus maintaining a high amount of active PCM inside it and preventing losses [21,22]. This type of incorporation is of particular interest due to its compatibility with the application of TES systems during the restoration and renovation of historical buildings. In previous works [17,23–25] the use of form-stable PCMs as aggregates for lime-based mortars has proven to be a suitable and sustainable solution to increase the thermal properties of the material. In their work, the authors proposed a vacuum impregnation method of PCM, i.e. PEG 1000 (Poly(ethylene glycol)), a non-toxic and non-flammable PCM, into a porous inorganic matrix, made of Lecce Stone obtained from waste material from the quarry, thus reducing further the environmental impact by re-integrating these waste material into the manufacturing cycle, considering the principles of circular economy [24]. The result is a *smart aggregate*, formally named Form-Stable Phase Change Material (FS-PCM), that provides thermal storage capacity to the mortar. The melting temperature of the PEG-1000 when introduced in the FS-PCM is in the range of 38–39℃ and a solidification temperature around 18–20℃ [24]. This makes them suitable to be applied in Mediterranean-like climates, e.g. regions where the summer conditions range from warm to hot and winter conditions are mild to cool (min temperatures typically above 0°C) [26], that given the current global climate crisis are not necessarily limited to the geographical Mediterranean region. One advantage of this type of composite system is that the specific transition temperatures can be selected simply by modifying the molecular weight of the PEG (Poly (ethylene glycol)) [23]. The thermal performance of the natural hydraulic lime mortars with the *smart* aggregates was found to decrease the need for heating during autumn and spring seasons, as well as reducing the requirement for cooling systems during summer [17]. In the case of winter, the results obtained for those mortars with PEG-1000 impregnated aggregates were not reported since the PCM was not activated at the studied temperatures, thus it was not possible to evaluate their performance.

The fresh properties of a mortar have an important influence on the hardened material. Particularly, the workability and water content of a mortar will determine its final physical properties, such as, e.g., the final mortar porosity or the binder-aggregate adhesion [27]. An excess of water in the mortar mixture can result on segregation, increment of porosity and overall, a reduced mechanical performance upon hardening.

In previous research [24], the fresh properties of mortars containing the *smart aggregates* were analyzed. It was observed that the presence of c.a 20 % of the *smart aggregates* in the mortar mixture increased the water requirement by 36 % with respect to a mortar without these aggregates. Thus, the presence of the aggregates of interest reduced considerably the workability of the mortar. Therefore, superplasticizers were then used to prepare the mortars. Using superplasticizers is a common solution to regulate the amount of water included in the mortar, to achieve the desirable workability. These materials are included in small quantities (less than 5 % w/w of the binder) and allow to reduce up to 40 % the water requirement of the mortar [28]. Despite the use of superplasticizers, the incorporation of FS-PCM aggregates into the lime-based mortar provoked a drastic reduction of the mechanical properties [24]. Both flexural and compressive strengths are dramatically reduced (by more than 50 %) with the introduction of the FS-PCM aggregates [24]. The inclusion of a superplasticizer helps to increase the mechanical performance; however, the flexural strength is reduced by 42 % and the compressive strength by 20 % [24]. Although it has not yet been proven, there are two main possible explanation of this: (i) a poor compatibility between the FS-PCM aggregates and the binder, and (ii) the dispersion of PCM from the aggregate into the mixture, thus changing the mechanical characteristics of the binder and of the mortar itself [23,29,30].

The dual aim of this work is to: a) verify the extension of the confinement of PEG-1000 inside the FS-PCM aggregates, and b) develop a methodology to prevent the migration and diffusion of PCMs that could limit the change of the mechanical properties of the considered lime mortars.

2. Materials and methods

2.1. Materials

The form-stable phase change material aggregates (FS-PCM) were obtained according to the procedure described by Frigione, et.al. [31]. The support matrix is Lecce stone, a miocenic calcarenite characteristic of the Salento Peninsula in the south of Italy [32] that was sieved to obtain a granulometry in the range of 1.6 – 2.0 mm. This natural stone is characterized by a generally homogeneous texture and a high open porosity [32] which makes it a good support for vacuum impregnation of the active PCM. The selected active PCM was Poly(ethylene glycol) (trade name PEG-1000) supplied by Sigma – Aldrich (Germany). This PCM has a melting point between 38°C and 39°C and a solidification temperature around 18–20°C [31], making it an appropriate phase change material to be used in warm climate regions. The final FS-PCM aggregates are constituted by 20 % by weight of PEG-1000 and 80 % of Lecce stone. Their granulometry remains between 1.6 and 2.0 mm.

The FS-PCM aggregates, thus obtained, were coated with five different materials: calcium hydroxide (CH), milk of lime (suspension of CH in water- M), natural hydraulic lime (NHL), cocciopesto (C), and pozzolana (P). The calcium hydroxide (CH), *Calce idrata Fiore di idrato purissimo extra ventilato*, and the natural hydraulic lime (NHL), *Calce Idraulica Naturale 3.5 ExNovo*, were provided by Fassa Bortolo Srl (Italy), whereas the cocciopesto (C), *Coccio pesto 1*, and pozzolana (P), *Pozzolana Romana Rossa Micronizzata*, were supplied by CTS company (Italy). All the materials were fine powders (granulometry bellow 0.2 mm).

Calcareous sands of two different granulometries (1.4–0.6 mm and 0.6–0.1 mm), supplied by Fassa Bortolo Srl, were used as aggregates in the mortar formulation to obtain a wider granulometric curve. The proportions of the dry components of the mix-design for the mortars are

reported in Table 1.

2.2. Modification of form stable phase change material aggregates

For the modification procedure to cover FS-PCMs, mineral materials (CH, M, NHL, C, and P) were applied following two different methods. For powder covering materials (CH, NHL, C and P) the FS-PCM aggregates were placed on a heating plate at 34°C under constant stirring (500–700 rpm). The heat allows to slightly melt the superficial PEG-1000 layer present in the aggregates. This superficial PEG-1000 will also work as kind of glue to promote the attachment of the powders to the surface. The powder coating materials were added exceeding the weight of the FS-PCM aggregates to be coated, and left under stirring for 20–30 min, until a homogeneous layer was observed in all FS-PCM aggregates. Finally, the coated aggregates (Fig. 1 CH, NHL, C and P) were left at room temperature to stabilize for 30 min before using them in the mortar preparation.

For the covering with milk of lime (M), the suspension made by 1 part of CH and 2 of distilled water, was applied by spraying at room temperature to FS-PCM aggregates until a homogeneous layer was observed. The aggregates were spread on a flat surface to avoid agglomeration. They were left to dry and carbonate for some hours and stored in glass containers at room temperature (Fig. 1 M).

The coating method produced grain particles of dimensions slightly larger than the uncoated FS-PCM. As a result, the new aggregates increment the granulometry 1.6 – 3 mm.

2.3. Mortar formulations (mix-design)

The mortar samples were prepared using hydrated lime and calcareous sand (supplied by Fassa Bortolo Srl), and *smart aggregates* based on Lecce stone (FS-PCM). The mortar formulation is reported in Table 1 and the same recipe is used for all sets of mortar specimens. The reported values correspond to the percentage by weight of the indicated dry materials (binder and aggregates). The total amount of distilled water added to the mixture was 33 % by weight of the total of dry components (i.e., the sum of all the weights added in the proportions expressed in Table 1). The mix design was selected to comply with the following constrictions: a. good workability in the fresh state, a binder to aggregate ratio between 1:2 and 1:3, water to binder ratio as close to 0.8, and with a maximization of the percentage of *smart* aggregates. To produce the mortars, first the dry components were mixed together to obtain a homogeneous distribution. Once all the dry components were mixed, the dry mixture was weighed and mixed with water, and then the fresh mixture was manually mixed. The fresh mortar mixture was purred in *ad-hoc* made molds (Fig. 2) using a metallic spatula. Once in the molds, the mixture was poked with a stick to remove the air bubbles present. Finally, the surface was flattened with a metallic spatula. All the mortars were cured in a controlled room at 20°C with 65 % RH for 11 days before removing the casts. After this period the mortars remained at room temperature and humidity to spontaneously carbonate for two months. Each set consist of 3 prismatic samples casted in molds of 5 ×25 x 100 mm^3 Fig. 2. This size allowed to have a reliable distribution of all the *smart* aggregates along at least two cartesian directions (XY), since two of the dimensions were at least 10 times larger than the maximum size aggregate (2 mm). Such reduced dimensions were selected because the standard prismatic molds require large quantities of material that that were not available for this work. In addition, when working with purely aerial lime mortars, it is extremely complicated to prevent cracking upon drying when using the standard prismatic molds. A possible way to prevent cracking, is the use of superplasticizers. However, they would have posed the problem of a potential FTIR signal overlapping with the PEG-1000. The specimen set with uncoated FS-PCM aggregates served as control, whereas the other sets were prepared with smart-aggregate modified as described in § 2.2.

Table 1
Proportions of the dry components of the mix-design for mortars with coated aggregates. The values are expressed in weight percentage.

Binder: Hydrated lime ($Ca(OH)_2$) % w/w	**Active aggregate** (FS-PCM, CH, M, NHL, C, P) % w/w	**Sand** (1.4–0.6 mm) % w/w	**Sand** (0.6 – 0.1 mm) % w/w	**Total of dry components % w/w**
30	40	20	10	**100**

2.4. Methods

2.4.1. Aggregates characterization

The microscopic characterization was performed on fragments and loose FS-PCM grains by stereomicroscopy (SM) using a Leica M205C microscope equipped with a Leica MC170 HD camera and on polished cross-sections of resin-embedded samples, using a Leica DM6 optical microscope (OM), with a 5x objective, coupled with a Leica Flexcam C1 camera in VIS light, these images were obtained using a dark-field filter.

The study of thermo-oxidation and quantification of the presence of PEG-1000 inside the aggregates was done with thermogravimetry analysis (TGA) using a Mettler-Toledo TGA/DSC. Each sample was subjected to a temperature raise from 25 to 950 °C at a heating rate of 20 K/min (50 mL/min) in air. In each measurement, c.a. 31 mg sample mass was pulverized in an agata mortar and placed into a ceramic crucible. The weight loss data was collected at regular time intervals.

Compositional mapping of the samples was performed on polished cross-sections using micro FTIR imaging (μ-FTIR) in total reflectance mode by a Thermo Nicolet iN10 MX spectrometer equipped with a cooled MCT/A detector. Mapping was performed using a detector aperture of 150 x 150 μm in areas of around 1.9×2.3 mm, with minimal variations depending on the morphology of the aggregate. On average 470 spectra were collected per area of analysis. The maps were obtained in the ultra-fast mode acquiring 1 scan per point in the mapped region. All scans were collected in the spectral range of 4000– 615 cm^{-1}. Consecutively, they were normalized and a selective intensity PCA mapping of the peak of interest corresponding to PEG-1000 was performed, using as reference peak 1960 cm^{-1} correlated to the crystallization state of PEG-1000 in its solid form [33,34].

Finally, to test the permanence of the coatings over the aggregates and the integrity of the coating, the aggregates were submerged in distilled water for 60 minutes under static conditions. Every 15 min, the aggregates were extracted and dried in room conditions for a day. The dried aggregates were observed with a stereomicroscope (SM) Leica M205C equipped with a Leica MC170 HD camera. The presence of PEG-1000 was analyzed via FTIR spectroscopy in attenuated total reflectance (ATR) mode using a NicoletTM iS20 spectrometer (ThermoFisherTM Scientific), equipped with a DTGS detector and a diamond itXTM Smart accessory for ATR in the spectral range 4000–400 cm-1, collecting 32 scans for each measurement with a 4 cm^{-1} spectral resolution (diameter of the crystal 2 mm).

2.4.2. Mortars characterization

For the characterization, fully carbonated mortar specimens were manually cut in prisms of approximately 5×5 ×25 mm^3 Fig. 2. A set of these prisms was used for TGA measurements. A second group used for FTIR powder analysis. A third set was embedded in resin and used for the microscopic imaging and μ-FTIR reflectance mapping. Finally, a last group of specimens was analyzed using X-Ray Micro Computed Tomography (μCT) and, subsequently, for the Mercury Intrusion Porosimetry (MIP) measurements.

The thermos-oxidation of the different mortars was performed using TGA in the same conditions as previously reported. Also, in this case a mortar sample was pulverized in an agata mortar and placed into the ceramic crucibles. The added material weighted on average 26 mg.

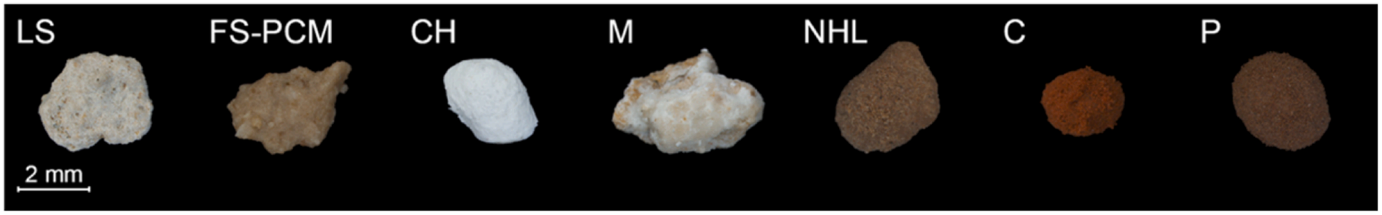

Fig. 1. Lecce stone aggregates (LS), and Form-Stable Phase Change Material (FS-PCM) aggregates coated with calcium hydroxide (CH), milk of lime (M), natural hydraulic lime (NHL), cocciopesto (C), and pozzolana (P).

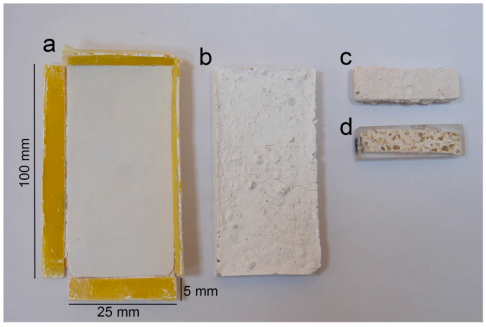

Fig. 2. (a) Mold of dimensions 5 x 25 x 100 mm^3 used to cast the specimens, (b) example of the full specimen obtained from the mold, (c) example of the cut specimen of approximate dimensions 5 ×5 x 25 mm^3 used for TGA, FTIR and X-Ray micro–Computerized Tomography (μCT) and MIP, and (d) example of specimen of approximate dimensions 5 ×5 ×25 mm^3 embedded in resin and used for μ-FTIR reflectance mapping.

A first evaluation of the coating efficacy was carried out analyzing the binder phase of the different mortar samples by FTIR spectroscopy in attenuated total reflectance (ATR) mode. The sampling powders were obtained from both cross section and the surface of the mortars. The measurements were made using the previously mentioned NicoletTM iS20 spectrometer (ThermoFisherTM Scientific).

The PEG-1000 dispersion in the mortars was evaluated using the μ-FTIR compositional mappings on polished cross-sections of resin-embedded samples. The acquisition conditions, normalization and PCA data processing were the same as those used for the characterization of the aggregates, however in this case the mapped areas were on average 1 cm^2 with an average of 11230 spectra collected.

To compare the presence of PEG-1000 in the mortars, image analysis in PCA intensity maps was performed. Selective pixel counting by color was done using Photoshop software for: blue, cyan, green, yellow, orange, and red pixels. In this case, blue pixels were considered indicative of the absence of PEG, whereas the sum of pixels cyan, green, orange, and red, accounted for the presence of PEG. The ratio between the pixels was done according to the following formula:

$$R = \frac{\sum C, G, O, \quad R}{B} \tag{1}$$

Where each initial letter indicates the pixel color considered (i.e.: cyan (C), green (G), orange (O), red (R), and blue (B)). Given this ratio R, the lower the value, the lower is the presence of PEG in the studied area. The described analysis was performed only on the areas where the impregnated Lecce stone aggregates were not present since they should contain PEG, and the interest was to evaluate the dispersion of PEG into the mortar. Therefore, considering these regions in the analysis may provide misleading results. The masking of the aggregates was performed with Photoshop software resulting in a layer where the FTIR PCA map was composed exclusively of the regions where the smart aggregates were not present.

The internal microstructure of the mortars was analyzed using X-Ray micro–Computerized Tomography (μCT) using a Xradia 510 Versa (Zeiss) equipment at the Centro de Instrumentación Científica (University of Granada, UGR), and a CoreTom (TESCAN) equipment at the Ghent University Core facility UGCT (the Centre for X-ray Tomography). Samples with CH and M coatings were analyzed in the Xradia μCT, whereas the mortars with control aggregates and coatings made of NHL, C, and P were analyzed in the CoreTom μCT scanner. All samples had a prismatic geometry with dimensions of 5 ×5 ×25 mm^3 and were analyzed in the conditions reported in Table 2. All data was analyzed using the Avizo3D (Thermo Scientific™) software. The studied mortars are composed by a binder phase and aggregates, some of which are porous by nature. Since the interest of the present study was to evaluate the internal porosity of the mortar excluding the contribution provided by the Lecce stone aggregates, it was necessary to exclude the porous aggregates. This was performed using two segmentations, one for the full set of pores present (A) and another for the porous aggregates (B), and then subtract them (A-B) to obtain a segmentation with only those pores and cracks present in the remaining mortar. This is schematized in Fig. 3. It is important to notice that this segmentation method is based on the grayscale selection of the areas of interest. In this case the grayscale of the image is equivalent to the intensities or attenuation coefficient of each material present, and it depends on their densities and elemental composition. This method is quite efficient; however, it has the limitation to do not fully differentiate regions with similar contrast due to both an artifact present in the tomography images and partial volume effect that overall makes the differentiation of small pores complicated. This can be solved using post-processing software, however in this work the marginal artefacts were not removed since the resulting errors caused in these samples were not significant. It would be desirable to eliminate phase bands from CT data and produce higher-quality data without artefacts that are easily segmented and quantified, but this requires more advanced post-processing software that was not available during the acquisition and analysis of the data. It can be also observed that also few non-porous aggregates may be partially marked in blue. However, for the scope of this work this was not considered relevant because the fundamental aspect was that the analysis program could efficiently mark the porous aggregates, since it is their porosity that needs to be subtracted from the total mortar porosity.

It is important to underline that the grayscale segmentation method inevitably introduces a systematic error, due to the already mention contrast artifacts and partial volume effect especially for those pores that are near the detection limit (8 μm and 9.7 μm depending on the Micro CT machine used). Moreover, all measured mortars are affected by the same systematic error, and thus this should not affect the comparison

Table 2
Operating conditions for the micro tomography scans in the two different equipment used.

Equipment	Magnification	Voltage (kV)	Power (W)	Binning	Resulting Voxel size (μm)
Xradia 510 Versa	0.4 X	60	5	1	9.7
CoreTom	37.5 X	120	15	2	8

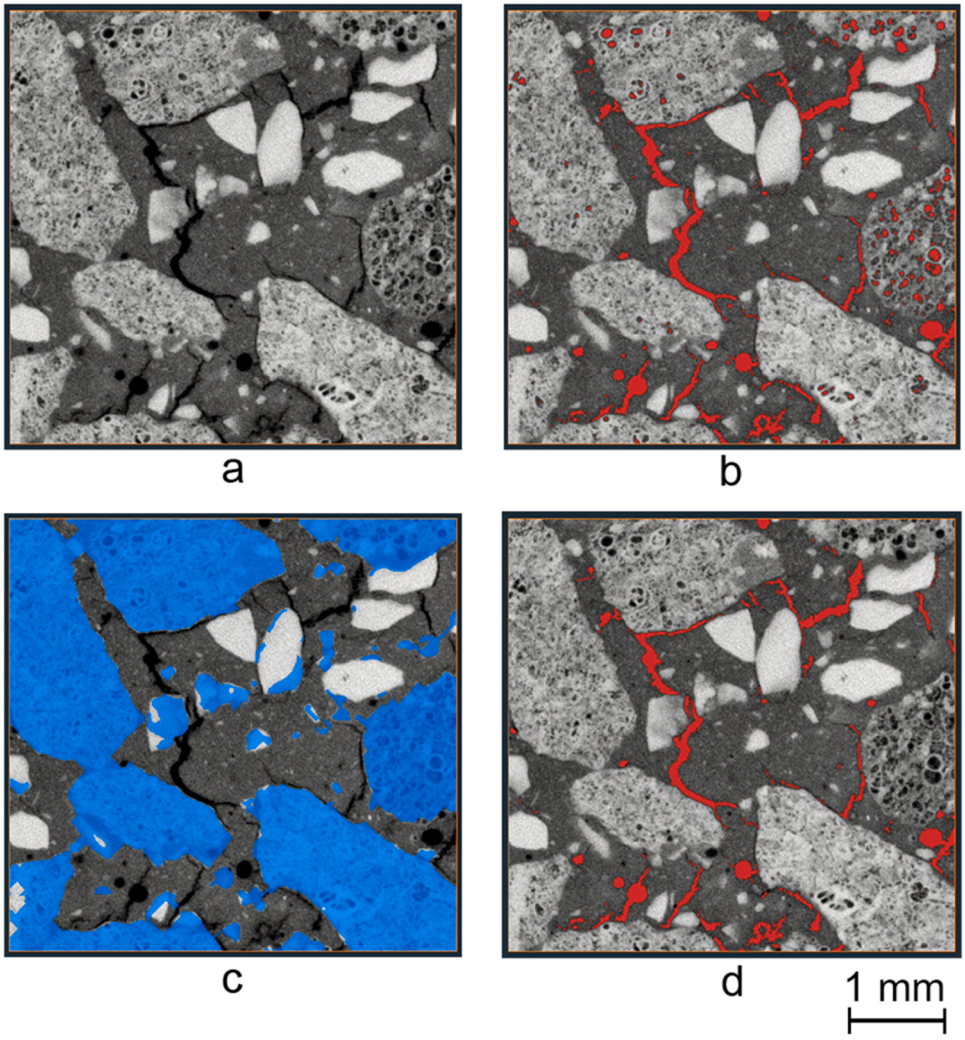

Fig. 3. Representative XY slides of the data processing of the micro tomography dataset using Avizo3D software: a) the original dataset; b) the first segmentation for the presence of pores in the whole mortar (in red all the pores are highlighted); c) the second segmentation exclusively for aggregate grains, mapped in blue; d) the final pore segmentation resulting from the subtraction of the aggregate grains from the original pore segmentation. This last segmentation results on the pores present only on the binder phase.

among them.

The porosity and pore size distribution were also determined via Mercury Intrusion Porosimetry (MIP) in a Autopore IV 9500 (Micromeritics) on mortar samples of approximately 3.5 g. All samples were dried in oven at 60°C until reaching constant weight, before porosimetric measurements.

3. Results and discussion

3.1. Characterization of the FS-PCM aggregates and evaluation of PEG confinement

The stereo-microscopic observation of the unmodified FS-PCM aggregates (Fig. 4) allows to observe that the Lecce stone aggregate grains show an external yellowish and *glossy* aspect. This is surely due to the presence of PEG-1000 over the surface of aggregates, because, during the impregnation process, the polymer that fills up the porosity of the stone grains, also covers the external surface. This observation and the reduction of surface roughness after the impregnation process were already reported in a previous paper [24]. It is possible that the superficial PEG-1000 covering the aggregate's surface might reduce the adhesion among binder and aggregates.

In the present work, the effect of liquid water on the FS-PCM aggregates has been investigated. The aggregate grains were immersed in distilled water for a period of 1 hour, and every 15 min a grain sample was extracted, dried and characterized by ATR-FTIR- spectroscopy, with the aim at evaluating the amount of PEG-1000. The results (Fig. 5) clearly indicate that, at increasing immersion times, a decrease of PEG-1000 peaks at 2880 cm^{-1} and 1100 cm^{-1} (due to C-H stretching

Fig. 4. optical micrography of a representative FS-PCM aggregate.

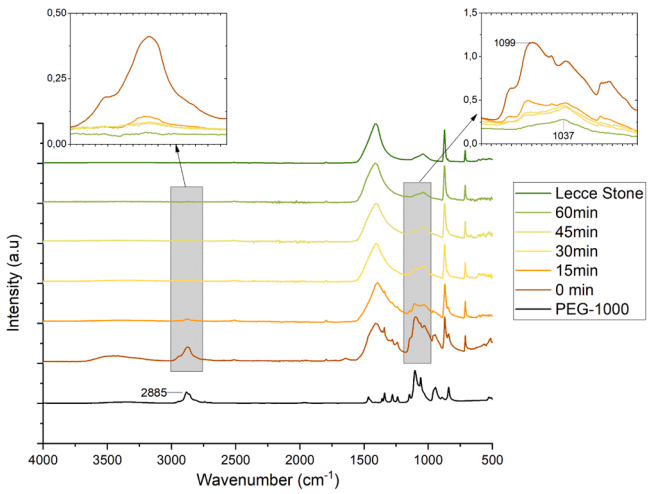

Fig. 5. FTIR spectra of the washing process under static conditions of the FS-PCM aggregates.

vibration and C-O-C vibration, respectively [35]), is observed. Moreover, after 30 minutes of water immersion, the presence of PEG-1000 is not detected anymore. Actually, PEG-1000 is a water-soluble polymer (50 mg/mL at 25°C): upon contact with water the external polymeric layer is readily dissolved, while for longer times, PEG-1000 diffuses from the porosity inside the stone aggregates into the surrounding liquid water.

Based on these results two main hypotheses can be formulated to explain the reduction of the mechanical properties of mortars:

i) The presence of PEG-1000 on the surface of the aggregate grains may hinder the correct mechanical interaction between the aggregate and the binder phases. This could prevent the suitable adhesion and interlocking forces from developing, and thus cause internal cracks and voids of the binder around the aggregates.
ii) When the fresh mortar mixture is prepared, the lack of confinement of PEG-1000 inside the FS-PCM grains, leads to the dissolution of the polymer into the liquid water and its diffusion into the mortar mixture and binder phase (up to now, the dispersion of PEG 1000 within the mortar and the related effects are not studied).

Evidently, it should also be considered that the reduction of the mechanical properties could be due to a combination of both hypotheses.

In any case, a possible solution for both hypothesized problems could be to cover the FS-PCM aggregates with a suitable layer of material with the aim of incrementing the compatibility and interaction between aggregate and binder phases. This cover should, at the same time, confine PEG 1000 inside the stone grains, reducing the contact of the polymer with water and, therefore, preventing the polymer diffusion and/or dispersion into the mortar. In the following sections the characterization and assessment of some proposed "coating" methodologies are presented and discussed.

3.2. Characterization of the modified FS-PCM aggregates

As reported in §2.2, the FS-PCM have been coated with a layer of different mineral materials, having high compatibility with both the lime binder and the Lecce stone aggregates: calcium hydroxide (CH), milk of lime (suspension of $Ca(OH)_2$ in water- M), natural hydraulic lime (NHL), cocciopesto (C), and pozzolana (P). All these materials are commonly used/added for the preparation of lime-based mortars since ancient times and should not negatively affect their properties, indeed some of them are added to improve the material. In Fig. 6 it can be observed that the coated aggregates are characterized by a layer of variable and not homogeneous thickness, depending on the different coating materials, ranging between 50 – 350 μm. Particularly, NHL presents the best structured coating with highest thickness, reaching over 350 μm in some areas. The coatings made with milk of lime (Fig. 6 M) and cocciopesto (Fig. 6 C) show the thinnest layers. The layer made with milk of lime is compact, thus potentially providing a higher degree of confinement, whereas that of cocciopesto has numerous regions of poor compactness. In this case, it is possible that the heterogeneous granulometry of the cocciopesto powder, in comparison with the other coating powders, reduces its covering capacity.

To assess the efficacy of the mineral covering in preventing PEG-1000 dispersion, both thermogravimetric analysis (TGA) and compositional mapping, by μ-FTIR reflectance spectroscopy, were performed on the aggregate samples. The TGA allowed to evaluate the content of PEG-1000 inside the aggregates, whereas the FTIR compositional mapping detected the PEG-1000 distribution inside the aggregate grains.

The TGA results (Fig. 7) revealed that the onset of PEG-1000 degradation process occurs for all samples at 325±1°C, in agreement with the onset of the reference PEG-1000 analyzed. In a previous work [24], the whole thermal degradation for these types of aggregates was observed between 218 and 297°C, however it is important to remark that these results were obtained in an inert atmosphere, while those

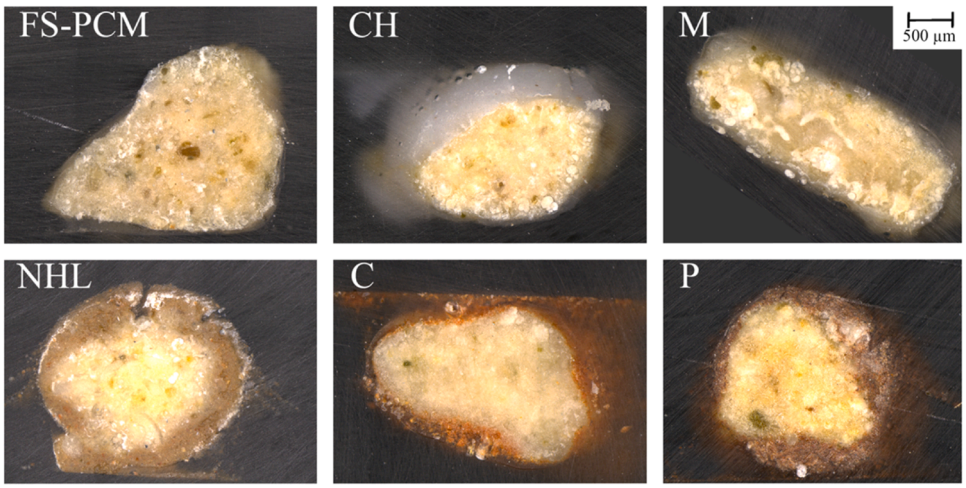

Fig. 6. Cross section micrographs of the, a) uncoated FS-PCM aggregates, and those coated with the five different materials: b) calcium hydroxide (CH), c) milk of lime (suspension of $Ca(OH)_2$ in water- M), d) natural hydraulic lime (NHL), e) cocciopesto (C), and f) pozzolana (P).

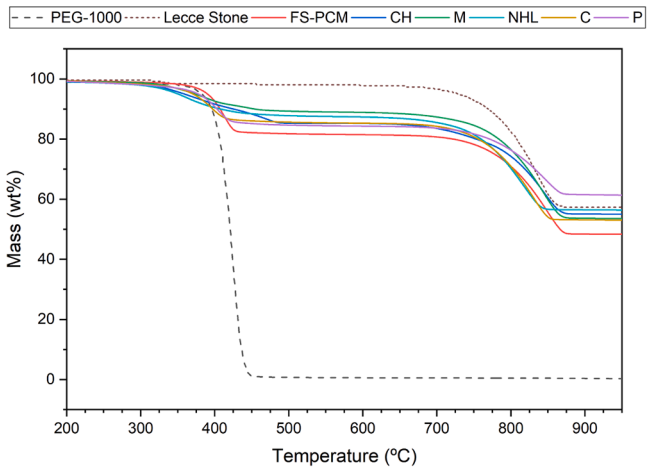

Fig. 7. Thermal degradation of the different coated aggregates with calcium hydroxide (CH), milk of lime (M), natural hydraulic lime (NHL), cocciopesto (C), and pozzolana (P)) and the reference uncoated aggregates (FS-PCM) in solid lines. The reference materials: Lecce stone (LS) and PEG-1000 in dashed lines.

presented in this work were performed on air. This is why a PEG-1000 reference was also analyzed in the same conditions as the *smart aggregates*. In the case of calcium hydroxide (CH) and milk of lime (M) coatings, the whole degradation process is prolonged to higher temperatures. The former is due to the contemporary degradation of calcium hydroxide ($Ca(OH)_2 \rightarrow CaO + H_2O$) which takes place in between 390 – 485°C [36] evidencing that the coating was not fully carbonated when the measurements were performed. Furthermore, the TGA allowed to quantify the effective amount of PEG-1000 in the aggregates. The amount of PEG-1000 inside each aggregate is reported in Table 3. The uncoated FS-PCM should contain approximately 20 % w/w of PEG-1000 [24]. The measured average weight percentage of the polymer in the coated aggregates is 11.80 %, this is because the coated aggregates are composed of three materials (the support Lecce stone, the PCM PEG-1000, and the mineral cover), thus for the same weight of sample, the relative TGA weight losses will be reduced for the coated aggregates with reference to the FS-PCM. Proof of this is that at 950ºC the residual material is higher for the coated aggregates. However, in the case of M coating (milk of lime, a suspension of Calcium hydroxide in water), the value is notably lower than the rest of the aggregates, this is possibly due to a partial PEG-1000 loss during the coating process, which is the only one that takes place in contact with water. Furthermore, the high percentage error associated with this measurement (M) is due to the previously mentioned contemporary degradation of $Ca(OH)_2$ and to the reduced amount of PEG-1000 present.

The distribution of PEG-1000 in the aggregates was also evaluated by μ-FTIR total reflectance mapping carried out on the coated FS-PCM cross sections. The results show that for the control FS-PCM aggregate (Fig. 8a), PEG-1000 is present mainly in the bulk of the aggregate, and on the external surface of the grain. The latter result is also confirmed by stereo microscopy observations of the uncoated aggregates (Fig. 4) where a PEG-1000 layer that covers the aggregate's surface can be observed. The aim of the coating process was to confine the PEG-1000 inside the Lecce Stone porous matrix to prevent its contact with the added water. As it can be seen, the results for the coated aggregates (Fig. 8b-f) reveal that in all cases it is possible to observe that PEG-1000 remains partly in the center of the aggregate, and concentrated within the coating layer. Although the PEG-1000 can be observed in the coating layer, this is mixed with the mineral covering, possibly lowering the risk of its dissolution in water and dispersion into the mortar.

Table 3
Weight percentages of PEG-1000 inside each aggregate. All the values are expressed in percentages.

FS-PCM	CH	M	NHL	C	P
17.24 ± 2.75	12.25 ± 2.27	8.40 ± 7.39	11.12 ± 3.72	13.04 ± 3.09	14.12 ± 1.50

To verify the coating's integrity under extreme conditions of water exposure, the aggregates were submerged under water for one hour and evaluated every 15 min. As it can be observed in Fig. 9, the coatings of calcium hydroxide (CH) and milk of lime (M) remain intact for the first 45 min. Instead, the other coatings (NHL, C and P) start to be dissolve during the first 15 min of immersion. This permanence capacity of the CH and M coatings is a positive sign of the coating capacity to reduce the PEG-1000/water interaction. In the case of hydraulic coatings (NHL, C and P), it should be possible to improve their resistance by carrying out a curing process at high humidities. Of course, it is important to remark that these are extreme conditions of water exposure, in the real scenario the aggregates would be exposed to a lime putty that may reduce the observed dissolution effect. FTIR results, indeed, indicate that, for all tested aggregates, there is a relevant dissolution effect, while, as will be shown in the following paragraph, there is a relevant confinement improvement once the aggregates are introduced into the mortar.

3.3. Characterization of the mortars

The TGA performed on the mortar specimens (Fig. 10) revealed similar results to those obtained for the aggregates. In this case the TGA revealed that each mortar contains on average 5.3 ± 0.6 % of PEG-1000, which is slightly lower than the theoretically calculated value of 8 % of PEG-1000 inside the mortars. Within these results, the PEG-1000 in the control mortar is always slightly higher than that of the other mortars, that contain a higher number of mineral components.

To evaluate the confinement capacity of coatings in the mortar specimens, two analyses were performed: ATR-FTIR spectroscopy on powders and Total Reflectance μ-FTIR mapping on polished cross-sections.

As can be observed in Fig. 11, in the case of the mortars made with uncoated FS-PCM (red line), there is a higher presence of PEG-1000 on/at the surface than in the center of the specimen. The latter is indicated by the stronger signal of the already mentioned peak at 2885 cm^{-1} and around 1100 cm^{-1} [35]. This evidences that the PEG-1000 is dissolved into water when the mortar is in the fresh state. Once the mortar is cast, it starts to dry, and the water evaporates moving towards the surface, carrying with it the dissolved PCM. The results observed in Fig. 11 highlight the capacity of the coating to reduce the contact of PEG-1000 with the fresh mortar water. The difference in the spectra presented for the mortars with pozzolana covered aggregates is due to its siliceous and aluminous nature, that indeed differs from the rest of the coating materials. In this case, Si-O-Si and Si-O-Al FTIR vibrations appear around 1050 cm^{-1} for the semi-crystalline or amorphous silica compounds.

Fig. 12 reports μ-FTIR compositional mapping of the different mortar specimens carried out on cross-sections. This allows comparing the effectiveness of the different mineral covers to confine the polymer inside the aggregates. When testing the FS-PCM control aggregates, the PEG-1000 can be observed both within the grains and all around in the binder regions, explaining the reported reduction of the mechanical properties [23,24,31]. On the contrary, when the aggregates are coated (Fig. 12 CH, M, NHL, C, and P) a confinement effect is evident, as the presence of PEG-1000 in the binder is drastically reduced. To evaluate the amount of polymer in the binder phase, image analysis was carried out based on selective pixel counting by color (§ 2.4.2). The ratio R (§ 2.4.2 Eq.(1)) was calculated for all mapped areas, excluding from this count the aggregates, where PEG-1000 is expected to be. For the measured ratio, lower values of R indicate a larger area of binder without PEG-1000 and therefore better confinement. In the case of the control mortars with uncoated FS-PCM $R_{FS\text{-}PCM}$ is 1.57, and for the mortars made with the different coated aggregates the ratios are as

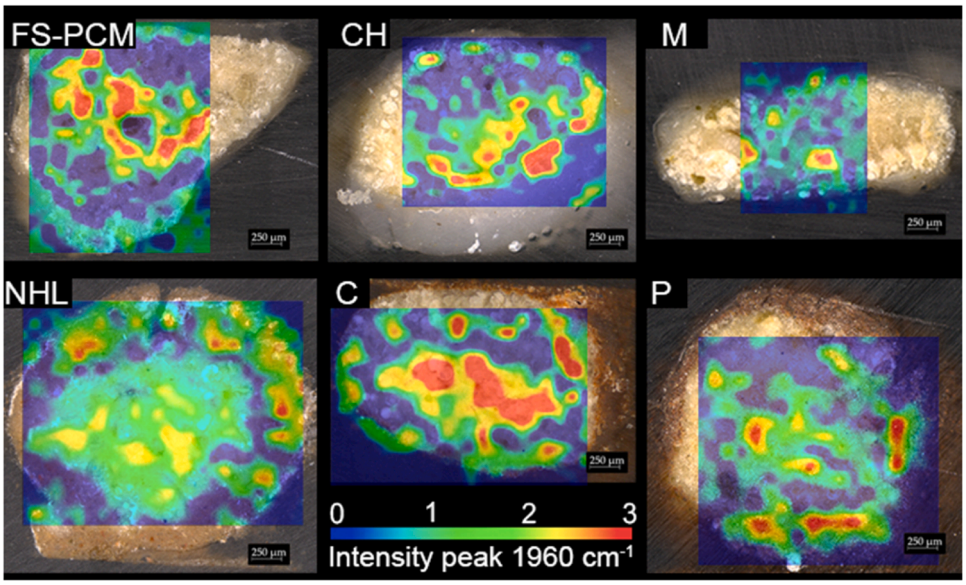

Fig. 8. PEG-1000 distribution maps of the FTIR signal reflectance intensity of the peak at 1960 cm^{-1} for each aggregate sample in a color scale where blue represents the absence of the signal and red its abundance. The reflectance maps of an uncoated FS-PCM, and coated with $Ca(OH)_2$ (CH), milk of lime (M), NHL, cocciopesto (C) and pozzolana (P) are presented.

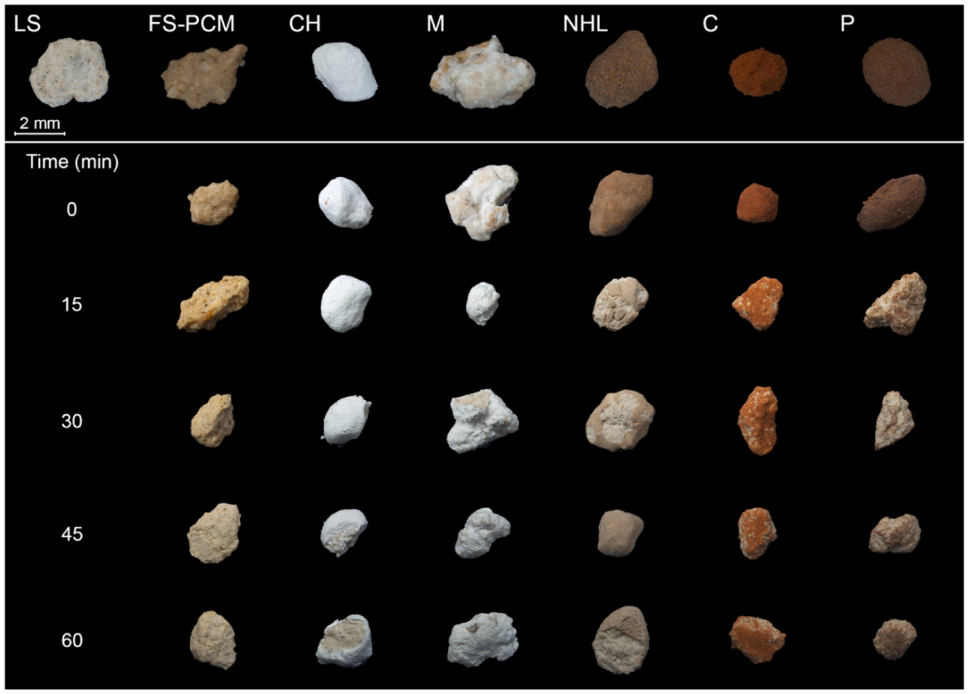

Fig. 9. Permanence of the coating made with Ca(OH)2 (CH), milk of lime (M), NHL, cocciopesto (C) and pozzolana (P) during 60 minutes of water immersion in stagnant conditions.

follows: $R_{CH} = 0.14$, $R_M = 0.27$, $R_{NHL} = 0.29$, $R_C = 2.58$, and $R_P = 0.35$. From this evaluation, all the coating materials except for cocciopesto coating, perform in a promising manner since all values are lower than the control one (1.57). The PEG-1000 confinement is improved by more than 77 % with respect to the mortar with uncoated aggregates. Particularly the CH cover seems promising, showing a 90 % improvement with respect to the control. In contrast, the mortars obtained with C covering fail to confine the PEG-1000. This poor result might be due to a scarce adhesion of cocciopesto to the grains, and rather inhomogeneous thickness Fig. 6).

The drastic reduction of the mechanical properties observed in the mortars realized with uncoated FS-PCM with respect to a mortar made with uncoated and non-impregnated aggregates [23] may be correlated as well to a higher degree of pores and internal cracks [37]. It is well known that there is a close relationship between the increment in the mechanical response of mortars and the reduction of cracks and porosity [38,39]. Therefore, evaluating the internal pore structure of the lime-based mortars with the modified aggregates is an important step on the assessment of the effectiveness of the mineral covering methodology. In general, the porosity of the mortars can be formed by elongated cracks or rounded pores [39]. Cracks can be created due to the shrinkage of the binder during setting and carbonation and depending on their size

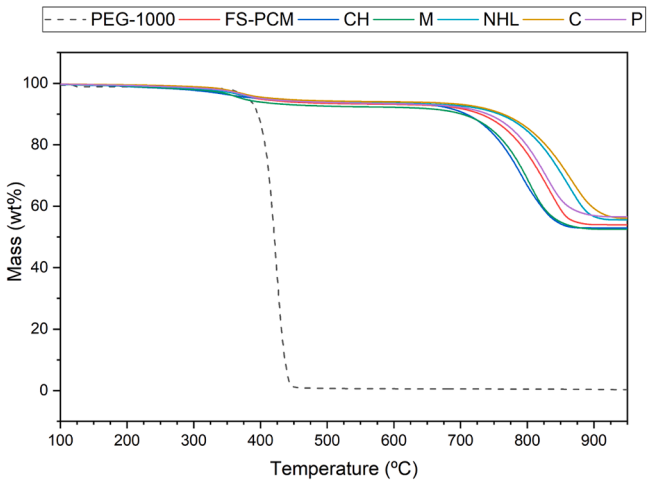

Fig. 10. Thermal degradation of the different mortar (solid lines) s realized with both uncoated FS-PCM aggregates and with the five different coated aggregates (calcium hydroxide (CH), milk of lime (M), natural hydraulic lime (NHL), cocciopesto (C), and pozzolana (P)) and the reference PEG-1000 (dashed lines).

they may have an impact on the mechanical properties of the mortar. In the present work, all the observed pores correspond to the macropore classification from the International Union of Pure Applied Chemistry (IUPAC), since they are all larger than 0.05 μm [40]. However, the pores ranging between 0.1 and 100 μm, are those mainly related to the water transfer properties of the mortar, while larger pores (above 100 μm in average diameter), also influence the mechanical resistance of the mortar, especially if they are interconnected [39,41].

Mercury Intrusion Porosimetry (MIP) and X-Ray Micro Computer Tomography (μCT) were used as complementary techniques to investigate the porosity and microcrack distribution inside the mortars. The MIP results can be observed in Fig. 13 and show the total porosity and pore-size distribution of the mortar specimens. The porosity of the mortars oscillates around 35.97 % ± 2.97 %, with the lowest value of porosity being that of the control mortar. This may be due to the partial dispersion of the PEG-1000 into the binder region. When all the water present has evaporated, the solid PEG-1000 will remain mixed with the binder at room temperature. The PEG will be located preferentially in the voids (pores and cracks) present in the binder. Moreover, those mortars with coated aggregates, show an increment of porosity in the range between 0.1 – 1 μm (Fig. 13) that may be related to the higher confinement, i.e. the lack of PEG-1000 in the binder.

The relative pores size distribution (Fig. 13) is similar for most of the mortars, with the highest number of pores in the diameter range 0.1 – 1 μm. Moreover, a similar distribution curve is observed for the natural Lecce stone grains [24]. This possibly indicates that a relevant contribution to the mortar's porosity is given by the presence of the Lecce stone aggregates. However, the MIP technique does not allow to differentiate between the mortar's pores and those in the Lecce stone aggregates.

Using the aggregates with coatings of NHL, cocciopesto and pozzolana allows for the reduction of pores with diameters larger than 10 μm, while increment those below 0.1 μm by at least 3 % compared to the control sample (Fig. 13). The hydraulic reactions may also consume some of the water present in the mortar creating some of the smaller pores. It is known that the hydraulic reactions tend to shift the porosity to smaller pore sizes [41,42]. It is worth noticing that to make the mineral covering, more than the necessary coating is added, and those mortars made with NHL, C and P change color from white to

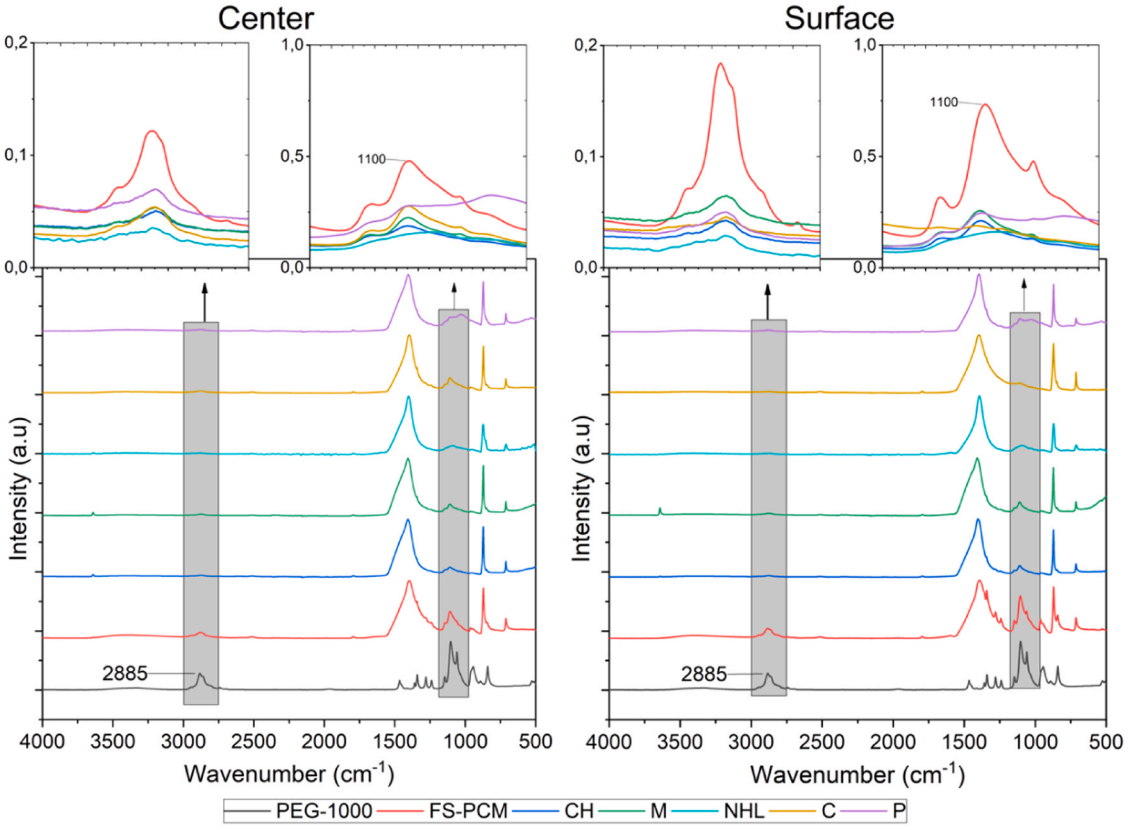

Fig. 11. Macro FTIR ATR mode of the powder sampled from both the center and the surface of the mortars made with the different aggregates (uncoated (FS-PCM), calcium hydroxide (CH), milk of lime (M), natural hydraulic lime (NHL), cocciopesto (C), and pozzolana (P)). The regions between 1200 – 1000 cm^{-1} and 2700 – 3000 cm^{-1} are highlighted in the insert graphs, where the characteristic vibrations of PEG-1000 are used as a reference for its presence.

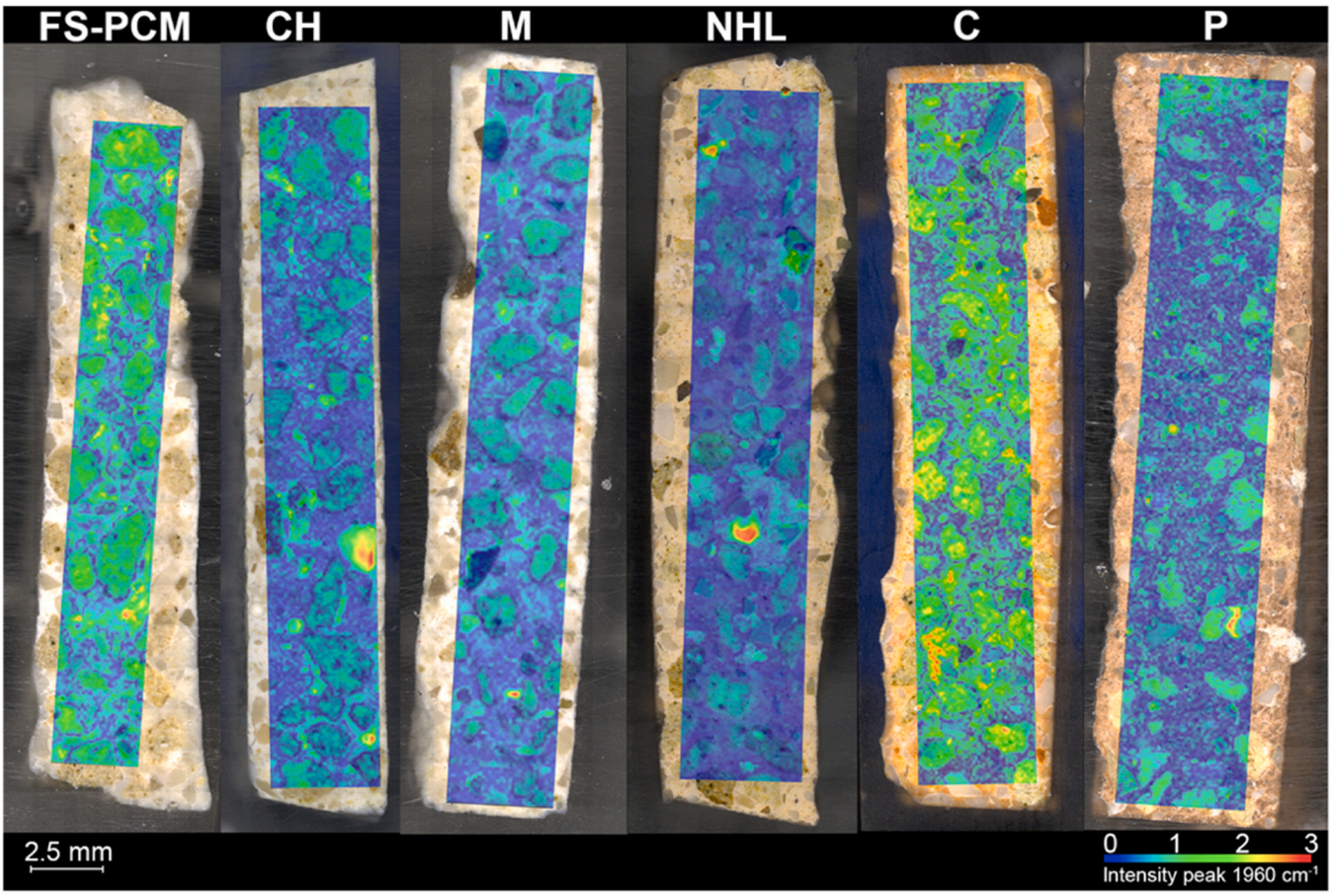

Fig. 12. PEG-1000 distribution maps of the FTIR signal reflectance intensity of the mortar samples in a color scale where blue represents the absence of the signal and red its abundance (a) uncoated FS-PCM, and coated with (b) (calcium hydroxide (CH), (c) milk of lime (M), (d) natural hydraulic lime (NHL), (e) cocciopesto (C) and (f) pozzolana (P).

brown/ochre according to the colors of the coating materials.

Finally, it must be underlined that MIP allows quantifying only the pores below 100 μm, but the larger pores and cracks, that are relevant for the mechanical properties of the mortars, are not observed with this technique.

X-Ray Micro Computed Tomography (μCT), on the other hand, allows to study the microstructure of the lime-based mortar and understand the interaction between the aggregates and the binder along the examined volume [41,43]. Moreover, this technique provides information on the internal porosity of the mortars at a larger scale than MIP, including voids larger than 100 μm, allowing to better infer the mechanical behavior of this material and, therefore, its general durability. It is, indeed, well known that, for ceramic porous materials, such as mortars, stones and concrete, the durability generally improves by reducing the porosity of the material [44,45]. In addition, normally, for porous materials with the same matrix and same pore-size distribution a larger porosity will lead to a lower mechanical resistance [46]. At the same time, for a porous material with the same matrix and the same total porosity, but with different pore-size distributions: the material with larger pores will result in lower mechanical resistance [46]. This is why, in lime-based mortars, macro pores are often correlated with the mechanical resistance of the bulk material. Particularly, the strength – macro porosity relationship for lime-pozzolan mortars was demonstrated to follow a power relationship where $S \propto (1-P)^n$, where S is the strength of the mortar and P is the porosity [47]. It is also important to remark that the features of interest (pores/voids) are larger than 19.4 μm, which is at least double in size of the voxel size used: 9.7 μm for XRadia 510 Versa and 8 μm for CoreTom. Furthermore, with this technique it is possible to selectively differentiate those voids present in the aggregates from those present in the binder phase, and segment them separately. In this way, it was possible to evaluate the porosity of the mortar excluding the porous aggregates (i.e., the binder region), which is of interest for this work. Therefore, in this case μCT was used to visualize and evaluate the structure and geometry of voids in the binder region. The images observed in Fig. 14 are representative 3D views of the voids, open and closed, of the binder region from two different mortar specimens: those made without any coating (FS-PCM) and the mortar made with calcium hydroxide coating (CH). Moreover, in Video 1 and Video 2 (S1 and S2 in supplementary material), the void network presented in Fig. 14 is displayed together with the whole analyzed volume of the mortar, thus allowing to further contextualize the studied voids in the presence of the other elements of the mortars. The μCT technique allows to also elucidate the complex interaction present in the interphase between the matrix and the porous aggregates. This problem might also be a consequence of the PEG-1000 diffusion in the binder phase, since it is localized in the border of the FS-PCM aggregates. The coating methodology helps to mitigate this, although it should be further optimized. As can be observed, the control mortar (FS-PCM) has a larger number of internal voids than the CH mortar. The segmentation of the binder's porosity revealed that the total volume occupied by pores and cracks is: 4.64 % for the FS-PCM (control), 2.71 % for CH, 1.75 % for M, 4.24 % for NHL, 3.73 % for C and 3.37 for P. Furthermore, the μCT images revealed that void regions found in the mortars with coated aggregates were primarily, not connected spherical pores, whereas for the control mortar with FS-PCM, both spherical pores and cracks were found along the whole examined volume. Also in this case, a porosity

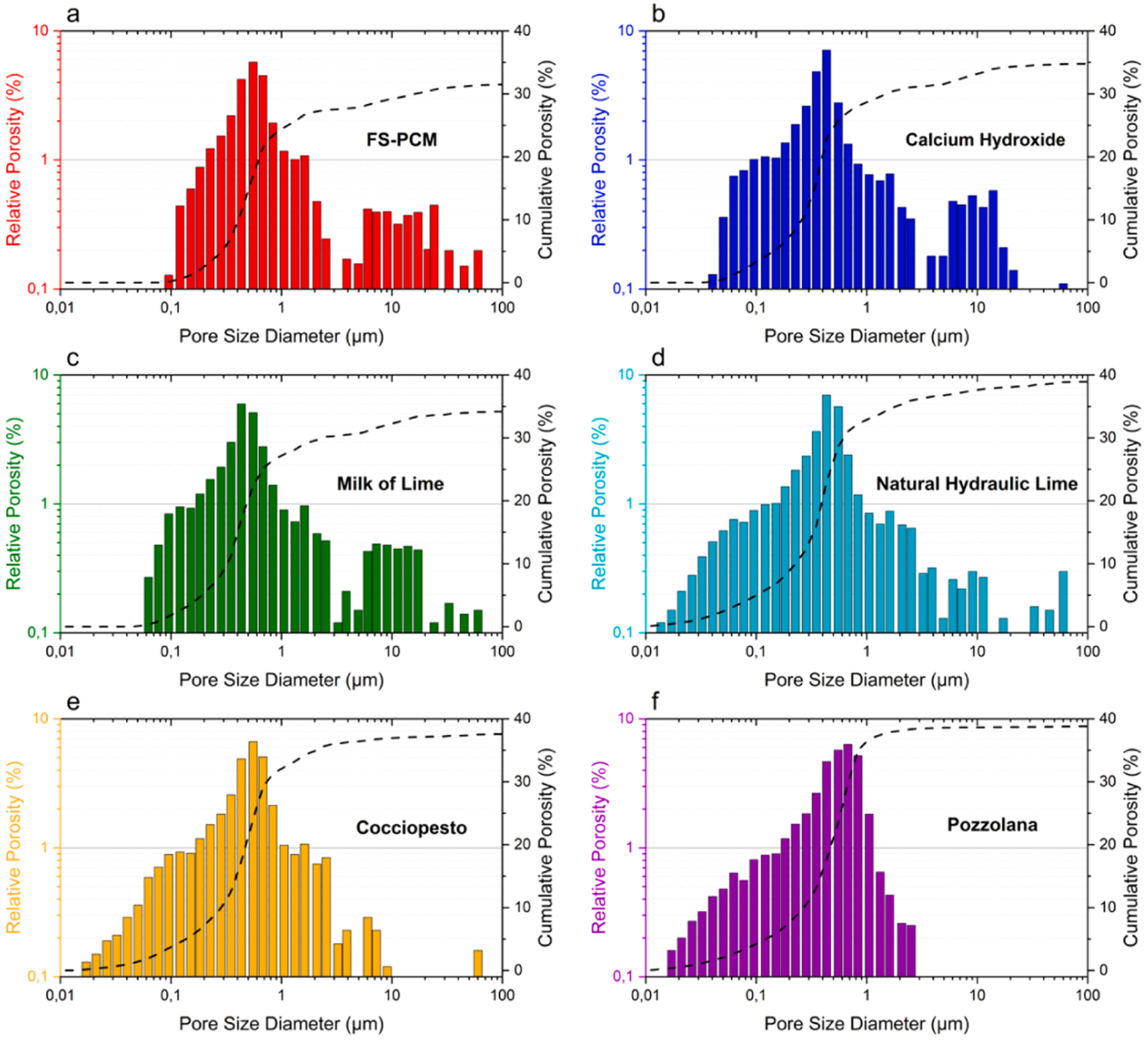

Fig. 13. MIP cumulative porosity percentage (dashed) and relative porosity percentage (bars) of lime-based mortars with different aggregates a) FS-PCM, and coated aggregates: b) Calcium Hydroxide (CH), c) Milk of Lime (M), d) natural hydraulic lime (NHL), e) Cocciopesto (C) and f) Pozzolana (P).

analysis was performed with the data obtained from the μCT. The results, shown in Fig. 15**,** highlight the reduction of the porosity when the coated aggregates are used in the mortars. Moreover, both M and CH covers perform the best in terms of total void volume and pore size reduction. This means that, when these coatings are used, the average diameter of voids tend to be smaller than 1 mm. This, should be considered the most relevant improvement, given that the control sample shows an average voids diameter over 3 mm. The coatings made with hydraulic powders has a lower impact on the void reduction, compared with CH and M. The reduction of pores and cracks observed with the μCT can be closely correlated to what it is observed in the compositional mapping. In the control mortar, where the PEG-1000 is not confined, this can be dispersed and mixed with the binder, possibly affecting the internal cohesion and interaction among mineral grains. Upon drying and hardening, a weakened binder will be more susceptible to internal cracks. These are the voids observed in the μCT experiment.

Supplementary material related to this article can be found online at doi:10.1016/j.conbuildmat.2024.138996.

In the present case, the matrix of all the tested mortars can be, to a first approximation, considered as similar, thus allowing to hypothesize the relative mechanical performance of the mortars based on their porosity. The use of coated aggregates, in most cases, reduces the total porosity of the mortars, and slightly shifts the pore-size distribution to smaller sizes. According to T. Lupin [46], both characteristics will have a positive impact on the strength of the mortars. In the present study, no mechanical testing of the mortars was performed due to a reduced availability of material. Although this study does not substitute the need for mechanical testing, it gives a first insight into the potential positive outcomes of the presented aggregate-coating methodology. To perform the mechanical testing, it was necessary to set up a new methodological approach that would allow to gain reliable information on the effect of PEG-1000 and rt aggregates even with the small quantities available. These experiments are currently ongoing and will be presented in future works.

4. Conclusions

The present investigation provided some light on the possible reason behind the relevant reduction of the mechanical properties of mortars made with FS-PCM, and proposed a novel methodology to prevent such

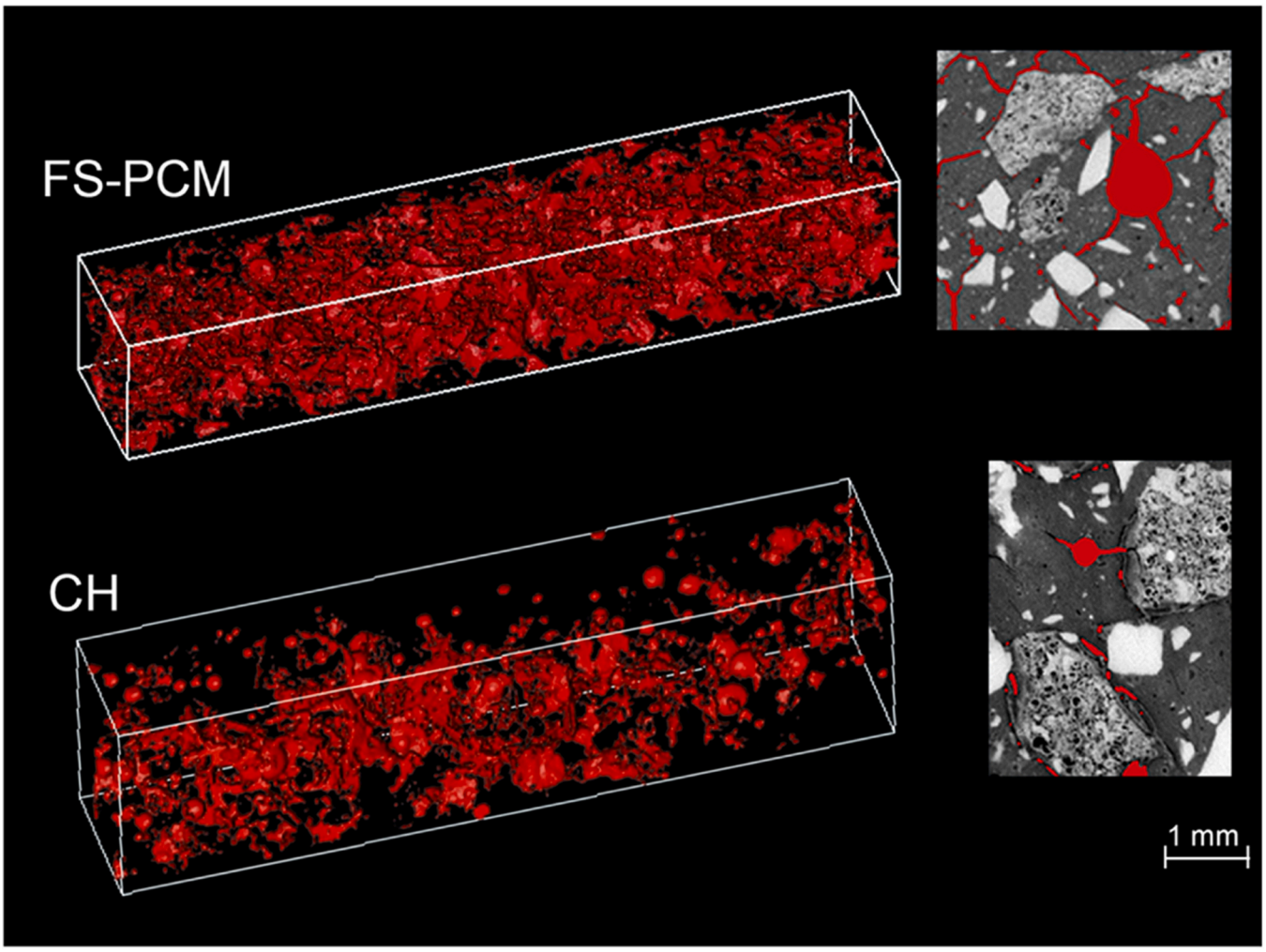

Fig. 14. Representative 3D view and XY slice of the binder pores and cracks present in uncoated FS-PCM, and the aggregate coated with Calcium Hydroxide (CH), the one with the highest porosity reduction. The volume corresponding to pores and cracks on the binder is highlighted in red, whereas the pores inside the aggregates are excluded, and thus not mapped in the presented image. Also, the grayscale image of the mortars is not included in this view to facilitate the visualization of the volume corresponding to the voids. The limits of the mortar's volume are delimitated in white.

problem. The poor confinement of PEG-1000 inside the FS-PCM aggregates and its consequent dispersion within the binder during the mixing stage of the mortar, has proved to be related to an increase of the porosity and cracks. PEG-1000 being highly soluble in water, is partially extracted from the aggregates and dispersed in the binder, where it could interfere between lime crystals and sand clasts, leading to weakening of the hardened material. To confirm this further research on the interaction between the PEG-1000 and the binder phase should be performed.

The proposed methodology for improving the PEG-1000 confinement inside FS-PCM aggregates consists of a simple mineral covering process of the aggregates with compatible materials: calcium hydroxide, milk of lime, natural hydraulic lime, cocciopesto, and pozzolana.

The results showed that the coating process, generally, does not affect the quantity of PEG-1000 inside the aggregates; only in the case of milk of lime, that requires a wet coating method, a partial loss of PEG-1000 is observed. Moreover, since the mineral cover adds a relevant quantity of material, for future tests of the mortar's thermal performance, the mix design needs to be adjusted to maintain the total quantity of active PCM constant.

When the coated aggregates are introduced in the mortar, the μ-FTIR compositional maps revealed a relevant reduction of PEG-1000 dispersion within the binder, compared to the control sample, the uncoated one. Results also show that the proposed cover methodology creates a thin layer around the aggregates. The coating thickness and its homogeneity depends on the type of applied material: this could be a problem since the efficacy of confinement may not be optimal in those regions where the thickness is lower. Therefore, as a future perspective, the coating methodology could be revised to optimize the cover-layer thickness and homogeneity. Moreover, data suggest that there is a partial dispersion of the coating within the mortar (e.g. slight color change with pozzolana and cocciopesto). The permanence of the coating material is an aspect that could be further investigated and optimized in the future to ensure that the coating remains surrounding the aggregates and is not dispersed in the mortar mixture.

The μCT porosity analysis revealed that total porosity and pore size distribution are reduced, giving rise to a higher degree of cohesiveness, and, therefore, potentially incremented mechanical properties. All mortars with coated aggregates showed an improvement both in terms of PEG-confinement and porosity reduction, except for the mortar with cocciopesto-coated aggregates that performed the worst. The overall assessment indicates that the coverings with calcium hydroxide and NHL are the most effective. Both materials are characterized by a good compatibility with aerial lime binder; in particular, NHL coating can also contribute to a further increase of the mechanical properties of the mortar, due to its hydraulic nature, and it is likely to perform even better when a NHL binder would be used in the mix-design.

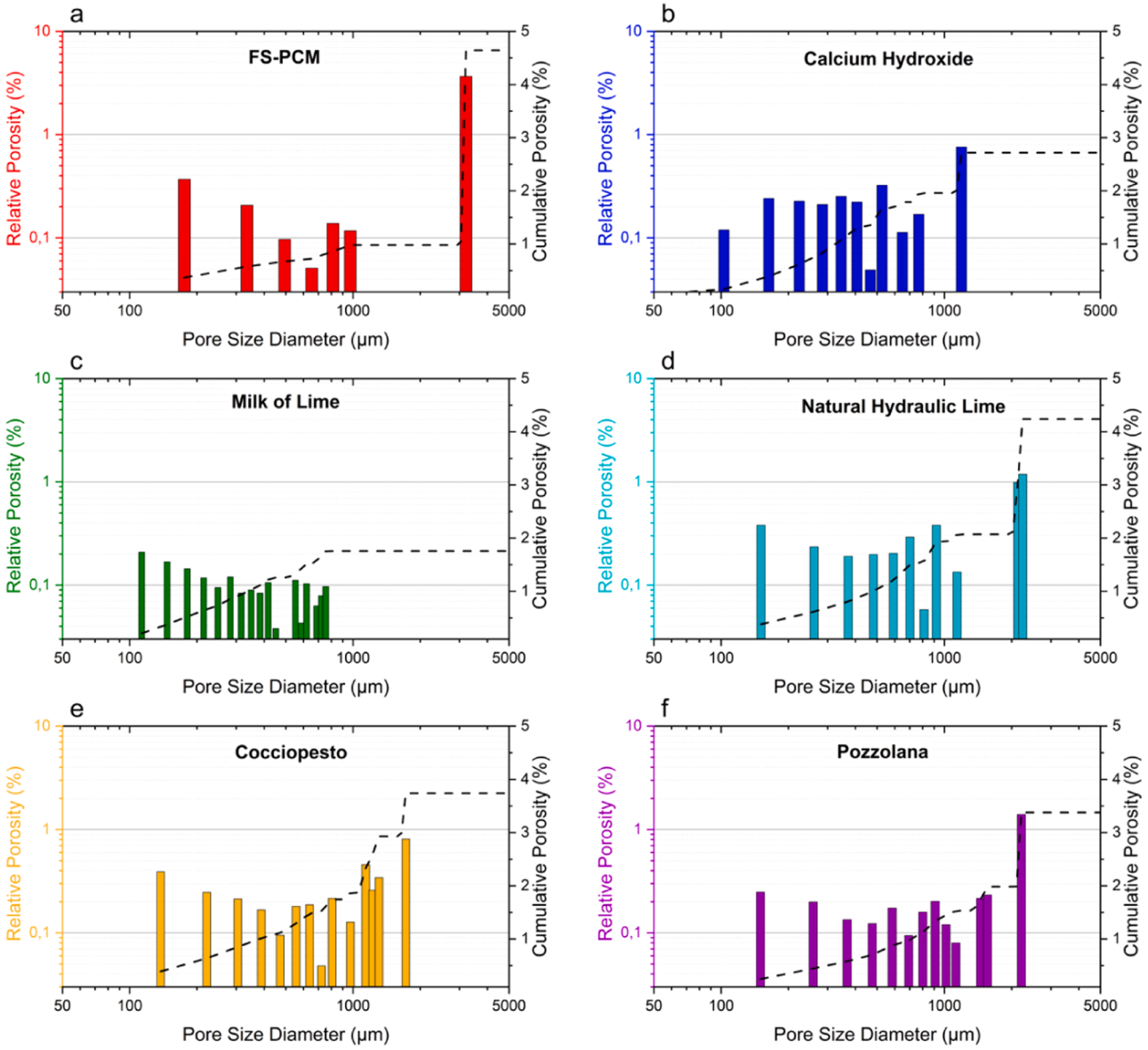

Fig. 15. Porosity analysis based on micro-CT data of lime-based mortars with different aggregates a) uncoated FS-PCM, and coated aggregates: b) Calcium Hydroxide (CH), c) Milk of Lime (M), d) NHL, e) Cocciopesto (C) and f) Pozzolana (P). The pores considered for this analysis are those found exclusively in the binder regions.

Ethical approval

The authors hereby state that the present work complies with ethical standards.

CRediT authorship contribution statement

Veerle Cnudde: Writing – review & editing. **Laurenz Schröer:** Writing – review & editing, Investigation, Data curation. **Sara Goidanich:** Writing – review & editing, Validation, Supervision, Resources, Project administration, Methodology, Funding acquisition, Conceptualization. **Lucia Toniolo:** Writing – review & editing, Validation, Resources, Funding acquisition, Conceptualization. **Mariaenrica Frigione:** Writing – review & editing, Resources. **Paulina Guzmán García Lascurain:** Writing – original draft, Visualization, Methodology, Investigation, Funding acquisition, Formal analysis, Data curation, Conceptualization. **Fátima Linares:** Writing – review & editing, Investigation, Data curation. **Antonella Sarcinella:** Writing – review & editing, Resources.

Declaration of Competing Interest

The authors declare the following financial interests/personal relationships which may be considered as potential competing interests: Paulina Guzman Garcia Lascurain reports financial support was provided by PON Ricerca e Innovazione 2014–2020. Paulina Guzman Garcia Lascurain reports financial support and travel were provided by EXCITE Network -European Union's Horizon 2020. Antonella Sarcinella reports was provided by PON Ricerca e Innovazione 2014–2020 Risorse React Eu. If there are other authors, they declare that they have no known competing financial interests or personal relationships that could have appeared to influence the work reported in this paper.

Aknowledgments

The present research was supported by the PhD Fellowship DOT1316197 (IMTR) CUP D45F21003710001 (Green) financed by Italian PON "Ricerca e Innovazione" 2014–2020 funding program. This research was partly supported by PON Ricerca e Innovazione

2014–2020 Risorse ReactEu - DM 1062/2021 Azione IV.4, “Dottorati e contratti di ricerca su tematiche dell’innovazione” and Azione IV.6, “Contratti di ricerca su tematiche green”.

The authors would like to thank the financing from the EXCITE network (projects COMPACT and SALSA), for the funding from the European Union’s Horizon 2020 research and innovation programme under grant agreement No 101005611 for Transnational Access conducted at University of Granada and Ghent University; The Centre for X-ray Tomography (BOF.COR.2022.0009) and IOF, project FaCT F2021/IOF-Equip/021 for CoreTom. Also, the authors would acknowledge Ghent University Special Research Fund (BOF-UGent) - BOF.COR.2022.0009.

The authors would like to thank Prof. Carlos Rodríguez-Navarro, Prof. Encarnación Ruíz Agudo, MSc. Alessandro Amendola and MSc. Elena Hitthaler for their help and advice. The authors also acknowledge the experimental support of Prof. Cristina Tedeschi, PhD. Mariagiovanna Taccia, PhD. Jorge Otero, PhD Liebert Parreiras Nogueira, MSc. Nicola Pinton, MSc. Francesco Santoro, MSc. Teodora Ilic, and MSc. Nicolò Guarnieri. Finally, the authors would like to thank Fassa Bortolo Srl for providing some of the materials used in this work.

Appendix A. Supporting information

Supplementary data associated with this article can be found in the online version at doi:10.1016/j.conbuildmat.2024.138996.

Data availability

Data will be made available on request. Micro CT data is available trough the YODA platform, Utrecht University, DOI: doi.org/10.24416/UU01-RTY94S

References

[1] United Nations Environment Programme, 2022 Global Status Report for Buildings and Construction: Towards a Zero-emission, Efficient and Resilient Buildings and Construction Sector, Nairobi, 2022.
[2] S.M. Fufa, C. Flyen, A.-C. Flyen, How can existing buildings with historic values contribute to achieving emission reduction ambitions, Appl. Sci. 11 (2021) 5978.
[3] U. Munarim, E. Ghisi, Environmental feasibility of heritage buildings rehabilitation, Renew. Sustain. Energy Rev. 58 (2016) 235–249.
[4] S.R.L. da Cunha, J.L.B. de Aguiar, Phase change materials and energy efficiency of buildings: a review of knowledge, J. Energy Storage 27 (2020) 101083, https://doi.org/10.1016/J.EST.2019.101083.
[5] M. Economidou, B. Atanasiu, C. Despret, J. Maio, I. Nolte, O. Rapf, J. Laustsen, P. Ruyssevelt, D. Staniaszek, D. Strong, Europe’s buildings under the microscope, A Ctry. Ctry. Rev. Energy Perform. Build. (2011).
[6] B. Lubelli, T.G. Nijland, R.P.J. van Hees, Characterization and compatibility assessment of commercial stone repair mortars, J. Cult. Herit. 49 (2021) 174–182, https://doi.org/10.1016/J.CULHER.2021.02.001.
[7] R. Veiga, Air lime mortars: What else do we need to know to apply them in conservation and rehabilitation interventions? A review, Constr. Build. Mater. 157 (2017) 132–140, https://doi.org/10.1016/J.CONBUILDMAT.2017.09.080.
[8] A. Isebaert, L. Van Parys, V. Cnudde, Composition and compatibility requirements of mineral repair mortars for stone – a review, Constr. Build. Mater. 59 (2014) 39–50, https://doi.org/10.1016/J.CONBUILDMAT.2014.02.020.
[9] R. Walker, S. Pavía, Thermal performance of a selection of insulation materials suitable for historic buildings, Build. Environ. 94 (2015) 155–165.
[10] M. Posani, R. Veiga, V.P. de Freitas, Retrofitting historic walls: Feasibility of thermal insulation and suitability of thermal mortars, Heritage 4 (2021) 2009–2022.
[11] L. Bianco, V. Serra, S. Fantucci, M. Dutto, M. Massolino, Thermal insulating plaster as a solution for refurbishing historic building envelopes: first experimental results, Energy Build. 95 (2015) 86–91.
[12] M. Posani, M.D.R. Veiga, V.P. de Freitas, Towards resilience and sustainability for historic buildings: a review of envelope retrofit possibilities and a discussion on hygric compatibility of thermal insulations, Int. J. Archit. Herit. 15 (2021) 807–823.
[13] A. Martínez-Molina, I. Tort-Ausina, S. Cho, J.-L. Vivancos, Energy efficiency and thermal comfort in historic buildings: a review, Renew. Sustain. Energy Rev. 61 (2016) 70–85.
[14] Z. Pavlík, A. Trník, M. Keppert, M. Pavlíková, J. Žumár, R. Černý, Experimental investigation of the properties of lime-based plaster-containing PCM for enhancing the heat-storage capacity of building envelopes, Int J. Thermophys. 35 (2014) 767–782, https://doi.org/10.1007/S10765-013-1550-8/FIGURES/14.
[15] S. Cunha, J.B. Aguiar, M. Kheradmand, L. Bragança, V.M. Ferreira, Thermal mortars with incorporation of PCM microcapsules, Restor. Build. Monum. 19 (2013) 171–178.
[16] T. Stahl, K.G. Wakili, S. Hartmeier, E. Franov, W. Niederberger, M. Zimmermann, Temperature and moisture evolution beneath an aerogel based rendering applied to a historic building, J. Build. Eng. 12 (2017) 140–146.
[17] A. Sarcinella, J.L.B. de Aguiar, C. Jesus, M. Frigione, Thermal properties of PEG-based form-stable Phase Change Materials (PCMs) incorporated in mortars for energy efficiency of buildings, J. Energy Storage 67 (2023) 107545.
[18] L. Liu, N. Hammami, L. Trovalet, D. Bigot, J.P. Habas, B. Malet-Damour, Description of phase change materials (PCMs) used in buildings under various climates: a review, J. Energy Storage 56 (2022) 105760, https://doi.org/10.1016/J.EST.2022.105760.
[19] P. Marin, M. Saffari, A. de Gracia, X. Zhu, M.M. Farid, L.F. Cabeza, S. Ushak, Energy savings due to the use of PCM for relocatable lightweight buildings passive heating and cooling in different weather conditions, Energy Build. 129 (2016) 274–283, https://doi.org/10.1016/J.ENBUILD.2016.08.007.
[20] Q. Al-Yasiri, M. Szabó, Incorporation of phase change materials into building envelope for thermal comfort and energy saving: a comprehensive analysis, J. Build. Eng. 36 (2021) 102122, https://doi.org/10.1016/J.JOBE.2020.102122.
[21] X. Wang, W. Li, Z. Luo, K. Wang, S.P. Shah, A critical review on phase change materials (PCM) for sustainable and energy efficient building: design, characteristic, performance and application, Energy Build. 260 (2022) 111923.
[22] P. Lv, C. Liu, Z. Rao, Review on clay mineral-based form-stable phase change materials: Preparation, characterization and applications, Renew. Sustain. Energy Rev. 68 (2017) 707–726.
[23] A. Sarcinella, J.Luís Barroso de Aguiar, M. Frigione, Physical properties of an eco-sustainable, form-stable phase change material included in aerial-lime-based mortar intended for different climates, Vol. 15, Page 1192, Materials 2022 15 (2022) 1192, https://doi.org/10.3390/MA15031192.
[24] M. Frigione, M. Lettieri, A. Sarcinella, J. Barroso de Aguiar, Sustainable polymer-based phase change materials for energy efficiency in buildings and their application in aerial lime mortars, Constr. Build. Mater. 231 (2020) 117149, https://doi.org/10.1016/J.CONBUILDMAT.2019.117149.
[25] A. Sarcinella, J.L.B. De Aguiar, M. Lettieri, S. Cunha, M. Frigione, Thermal performance of mortars based on different binders and containing a novel sustainable phase change material (PCM), Vol. 13, Page 2055, Materials 2020 13 (2020) 2055, https://doi.org/10.3390/MA13092055.
[26] A. Sarcinella, J.L.B. de Aguiar, C. Jesus, M. Frigione, Thermal properties of PEG-based form-stable Phase Change Materials (PCMs) incorporated in mortars for energy efficiency of buildings, J. Energy Storage 67 (2023) 107545.
[27] R. Hanley, S. Pavía, A study of the workability of natural hydraulic lime mortars and its influence on strength, Mater. Struct. Mater. Et. Constr. 41 (2008) 373–381, https://doi.org/10.1617/S11527-007-9250-0/TABLES/6.
[28] B. Silva, A.P.F. Pinto, A. Gomes, A. Candeias, Fresh and hardened state behaviour of aerial lime mortars with superplasticizer, Constr. Build. Mater. 225 (2019) 1127–1139.
[29] S. Cunha, A. Sarcinella, J. Aguiar, M. Frigione, Perspective on the development of energy storage technology using phase change materials in the construction industry: a review, Energies 16 (2023) 4806.
[30] P.Guzman Garcia Lascurain, A. Amendola, M. Frigione, A. Sarcinella, L. Toniolo, S. Goidanich, Optimization of eco-sustainable, form-stable phase change material to be incorporated in aerial-lime- based mortars, Int. Congr. Polym. Concr. (ICPIC), Wars. (2023).
[31] M. Frigione, M. Lettieri, A. Sarcinella, J.L.B. de Aguiar, Applications of sustainable polymer-based phase change materials in mortars composed by different binders, Vol. 12, Page 3502, Materials 12 (2019) 3502, https://doi.org/10.3390/MA12213502.
[32] A. Calia, M. Laurenzi Tabasso, A. Maria Mecchi, G. Quarta, The study of stone for conservation purposes: Lecce stone (southern Italy), Geol. Soc. Lond. Spec. Publ. 391 (2014) 139–156.
[33] P. Li, J. Wu, S. Hao, Z. Lan, Q. Li, Y. Huang, Quasi-solid state dye-sensitized solar cells based on the cross-linked poly (ethylene glycol) electrolyte with tetraethoxysilane, J. Appl. Polym. Sci. 120 (2011) 1752–1757.
[34] D.H. Doshi, W.R. Ravis, G.V. Betageri, Carbamazepine and polyethylene glycol solid dispersions: preparation, in vitro dissolution, and characterization, Drug Dev. Ind. Pharm. 23 (1997) 1167–1176.
[35] B. Kalidasan, A.K. Pandey, R. Saidur, B. Aljafari, A. Yadav, M. Samykano, Green synthesized 3D coconut shell biochar/polyethylene glycol composite as thermal energy storage material, Sustain. Energy Technol. Assess. 60 (2023) 103505.
[36] Q.T. Phung, N. Maes, S. Seetharam, Pitfalls in the use and interpretation of TGA and MIP techniques for Ca-leached cementitious materials, Mater. Des. 182 (2019) 108041.
[37] V. Brunello, C. Canevali, C. Corti, T. De Kock, L. Rampazzi, S. Recchia, A. Sansonetti, C. Tedeschi, V. Cnudde, Understanding the microstructure of mortars for cultural heritage using X-ray CT and MIP, Materials 14 (2021) 5939.
[38] M. Arandigoyen, J.I. Alvarez, Pore structure and mechanical properties of cement–lime mortars, Cem. Concr. Res 37 (2007) 767–775.
[39] S. Maria, Methods for porosity measurement in lime-based mortars, Constr. Build. Mater. 24 (2010) 2572–2578.
[40] D.H. Everett, Manual of symbols and terminology for physicochemical quantities and units, appendix II: definitions, terminology and symbols in colloid and surface chemistry, Pure Appl. Chem. 31 (1972) 577–638.
[41] S.D. Rani, A.V. Rahul, M. Santhanam, A multi-analytical approach for pore structure assessment in historic lime mortars, Constr. Build. Mater. 272 (2021) 121905.

[42] C. Nunes, Z. Slížková, M. Stefanidou, J. Němeček, Microstructure of lime and lime-pozzolana pastes with nanosilica, Cem. Concr. Res 83 (2016) 152–163.
[43] R. Travincas, M.F.C. Pereira, I. Torres, A. Mauricio, D. Silveira, I. Flores-Colen, X-ray microtomography applied to mortars: Review of microstructural visualization and parameterization, Micron 164 (2023) 103375.
[44] L. Bertolini, B. Elsener, P. Pedeferri, E. Redaelli, R.B. Polder, Corrosion of steel in concrete: prevention, diagnosis, repair, John Wiley & Sons, 2013.
[45] C. Groot, R. Veiga, I. Papayianni, R. Van Hees, M. Secco, J.I. Alvarez, P. Faria, M. Stefanidou, RILEM TC 277-LHS report: Lime-based mortars for restoration–a review on long-term durability aspects and experience from practice, Mater. Struct. 55 (2022) 245.
[46] T. Luping, A study of the quantitative relationship between strength and pore-size distribution of porous materials, Cem. Concr. Res 16 (1986) 87–96.
[47] I. Papayianni, M. Stefanidou, Strength–porosity relationships in lime–pozzolan mortars, Constr. Build. Mater. 20 (2006) 700–705.